

Large-scale cortical displacement of a human retinotopic map

Scott D. Slotnick,^{CA} Lauren R. Moo,¹ Gregory Krauss¹ and John Hart Jr^{1,2,3}

Departments of Psychology,¹ Neurology,² Cognitive Science, and ³F.M. Kirby Center for Functional Brain Imaging, Johns Hopkins University, 3400 North Charles Street, Baltimore, MD 21218, USA

^{CA}Corresponding Author

Received 11 October 2001; accepted 5 November 2001

The aim of the current study was to determine the retinotopic organization of a patient with congenital cortical dysgenesis and normal visual function. Using functional magnetic resonance imaging (fMRI), detailed retinotopic maps corresponding to the four visual field quadrants were projected onto cortical surfaces. Similar to control subjects, the upper right visual field mapped onto ventral left hemisphere and was retinotopically organized. The lower right visual field's cortical representation was also retinotopically

organized, yet was displaced many centimeters anteriomedially. Moreover, the entire left visual field was represented in non-retinotopically organized islands in both hemispheres. These results indicate retinotopic maps can shift in both location and topography illustrating cortical reorganization presumably due to either cortical dysgenesis or functional displacement. *NeuroReport* 13:41–46 © 2002 Lippincott Williams & Wilkins.

Key words: Cortex; Extrastriate; fMRI; Human; Plasticity; Reorganization; Retinotopic map; Retinotopy; Striate; Vision

INTRODUCTION

Patients with chronic lesions have demonstrated the capacity for cortical reorganization. Tumors located in the area of motor cortex dedicated to hand movements have been shown to shift the cortical representation of the hand

several centimeters [1,2]. Patients with arteriovenous malformations (AVMs), a congenital abnormality, in either the foot or hand region of primary motor cortex show no deficit in movement, but a shifted cortical motor representation either within primary motor cortex or extending into

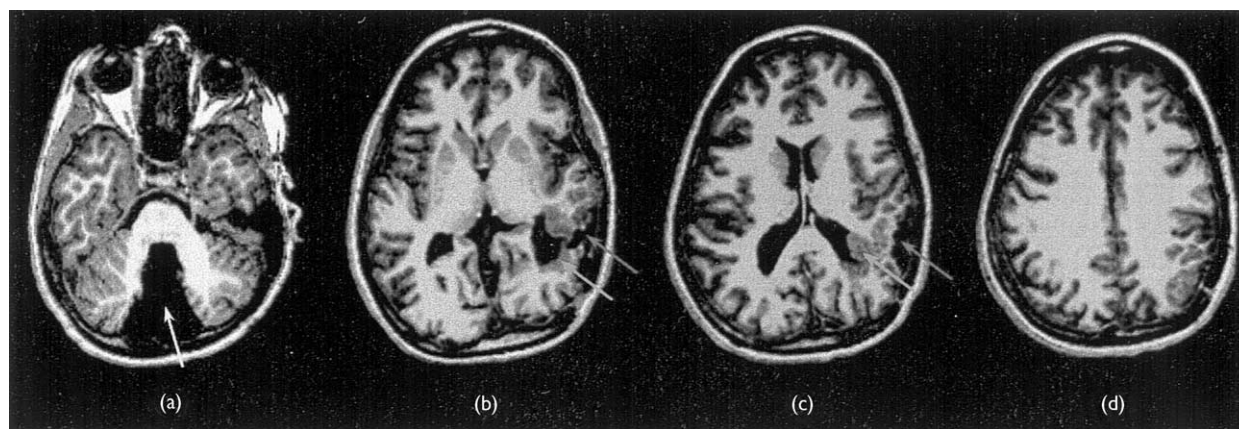


Fig. 1. Axial slices, inferior to superior, through high-resolution anatomic MRI parallel to AC-PC line and perpendicular to mid-sagittal plane (left hemisphere on left). For all slices, visual areas are located on the medial posterior cortical surface. (a) Inferior slice through cerebellum with enlarged fourth ventricle, illustrated by arrow, indicative of a Dandy-Walker malformation. (b) Slice through ventral extrastriate visual areas. On this and the next slice, solid arrow indicates right hemisphere peri-ventricular heterotopia and dotted arrow indicates the locus of gray/white matter surgical excision to relieve seizures. Note global cortical dysgenesis of both hemispheres. (c) Slice through VI. Note absence of right hemisphere white matter near tip of solid arrow, which would typically contain optic radiations from lateral geniculate nucleus to VI carrying information from left visual field. (d) Slice through dorsal extrastriate visual areas.

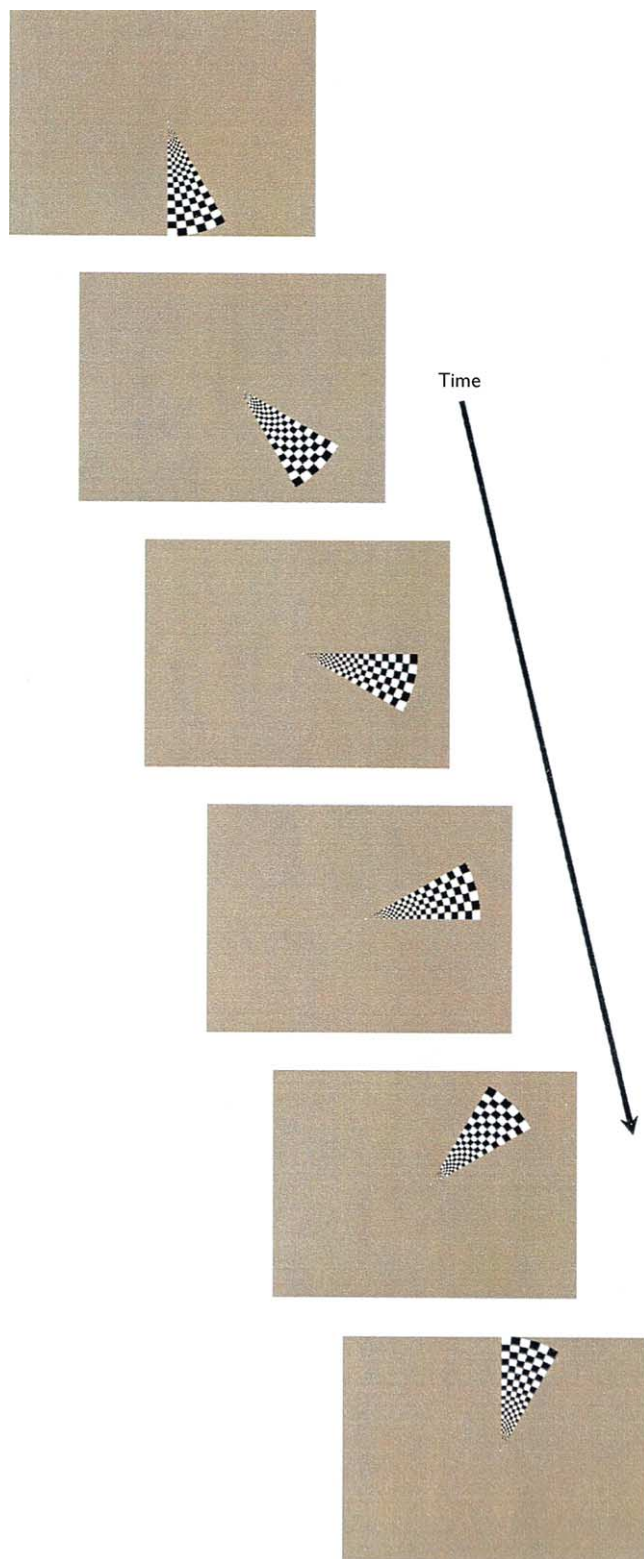


Fig. 2. Snapshots of the rotating stimulus wedge, extending from 0.3 to 6.8° visual angle from fixation with 30° polar angle width, used for retinotopic mapping of the right visual field. The stimulus wedge began at $t = 0$ s with its leading edge abutting the upper vertical meridian, then rotated counterclockwise continuously with a cycle time of 72 s. The left visual field is stimulated similarly during the first half of the cycle.

non-primary motor cortex [3]. Similarly, a group of patients with AVMs in typical left hemisphere cortical language areas have shown a shift of language representation to the right hemisphere [4,5]. In the visual domain, congenitally blind subjects have been shown to activate visual cortex in response to Braille reading indicating that this region may be recruited by somatosensory cortex [6].

Human cortical retinotopic maps across normally-sighted individuals have been shown to be extremely similar in both their location relative to anatomical landmarks and their overall topography [7–10]; however, little is known of their capacity for reorganization. Although a recent study has shown retinotopic map reorganization to some degree [11], advances in human retinotopic mapping now allow the detailed study of retinotopic reorganization to the resolution of the early visual area (e.g. V1, V2, V3, VP, V3A, and V4v).

If a lesion were to disrupt, either anatomically or functionally, the area of cortex normally containing a retinotopic map, at least three non-exclusive hypotheses exist regarding the possible resultant cortical reorganization. First, a large-scale shift in the retinotopic map to preserved cortex may occur *in toto* (i.e. retaining topographic organization overall). Second, the retinotopic map may shift to a different cortical location retaining its contiguity but losing its topographic organization. Third, a shift in both location and topography may occur resulting in map represented by numerous spared cortical loci with disorganized topography. In contrast to the hypotheses relating to cortical reorganization, the null hypothesis is that the retinotopic map is fixed in its normal location/topography such that disrupted cortex would result in a visual field deficit. The current study uses detailed retinotopic mapping techniques to explore these hypotheses in a patient with significant congenital cerebral dysgenesis.

MATERIALS AND METHODS

The patient was a 32-year-old left-handed woman originally diagnosed with hemispheric cerebral dysgenesis as illustrated by a thick periventricular band heterotopia and a Dandy-Walker malformation (Fig. 1). She underwent a partial right temporal lobectomy at age 30 for treatment of medically intractable seizures. Detailed perimetry mapping within the central 60° of the visual field revealed normal visual function.

During the entire experimental session, the patient was alert, pleasant in manner, and in no apparent distress. After the nature of the experiment was fully explained and comprehended by the patient, informed consent was obtained. The experimental protocol had been approved by the Johns Hopkins Hospital internal review board. The stimulus was similar to those used in other fMRI human retinotopic mapping studies [7–10]. As increases in fMRI blood oxygen level dependent (BOLD) signal changes have been directly and indirectly correlated with neural activity in non-human primate and human [12–15], it was assumed that fMRI signal changes reflect neural activity. In the present study, the rotating checkerboard stimulus wedge reversed in contrast 8 times/s and completed eight cycles in a total of 9 min 42 s (Fig. 2).

Individual squares comprising the wedge were scaled by the human cortical magnification factor [15]. Throughout

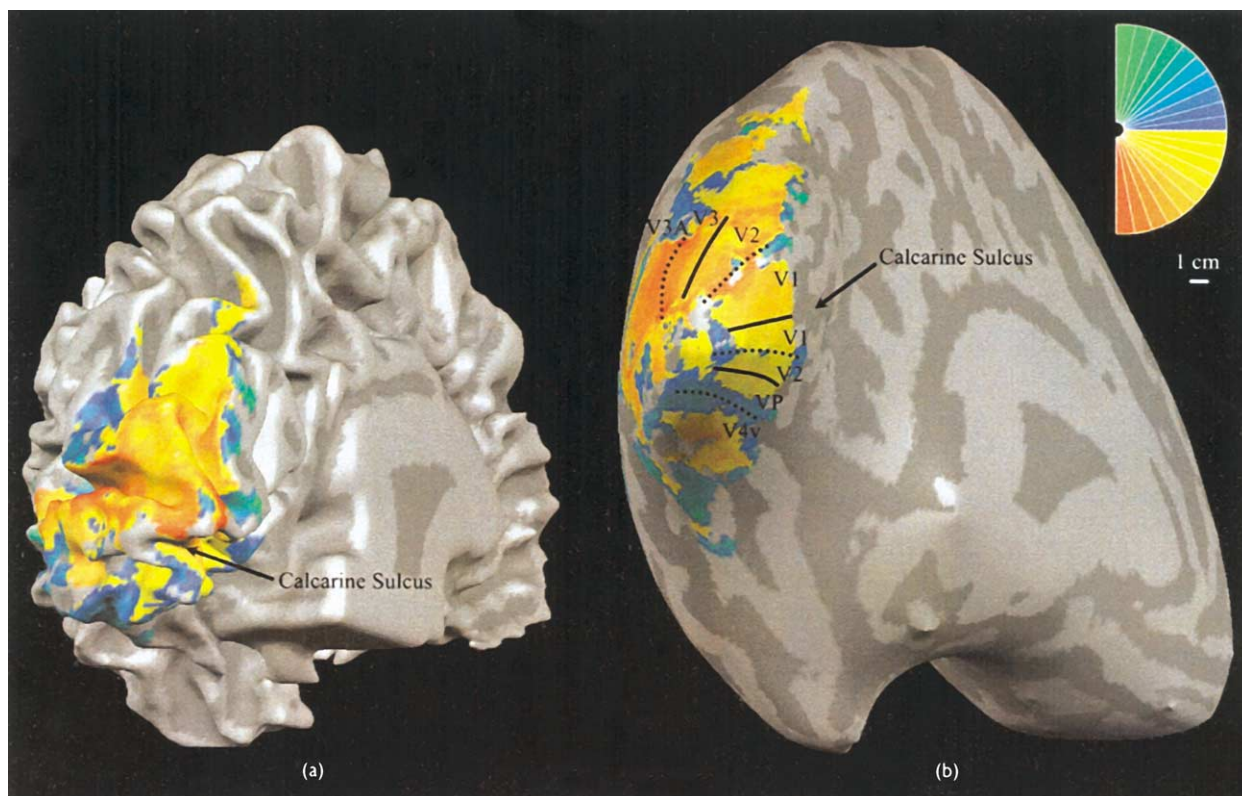


Fig. 3. (a) Retinotopic map of right visual field projected onto left hemisphere of a control subject. Gyri are colored light gray, sulci dark gray, and active voxels corresponding to unique visual field locations are colored according to colorwheel shown to upper right. (b) Identical retinotopic map projected onto inflated representation of the cortical surface with early visual areas identified. Horizontal meridian representations are indicated by solid lines and vertical meridian representations are indicated by dotted lines.

the experimental run, the patient was instructed to maintain central fixation and press a button with her right thumb when a randomly selected square in the display flashed red for 120 ms. Such targets occurred on average every 15 s.

Images were acquired using a 1.5T Philips Gyroscan ACS-NT scanner with either a Philips end-capped quadrature birdcage head coil (anatomic scan) or a Phillips circular C3 surface coil (functional scan). Following a T1-weighted scout image, the high-resolution anatomic images were acquired using an MPRAGE sequence (echo time (TE) = 3.7 ms, flip angle = 8°, time of repetition (TR) = 8.1 ms, number of excitations = 1, 256 × 56 matrix, 256 × 256 mm field-of-view (FOV), 256 × 1 mm slices, no gap, i.e. 1 mm isovoxel resolution). T2*-weighted functional data were acquired using echo-planar imaging (TE = 40 ms, flip angle = 90°, phase-encoding = foot-to-head, TR = 3000 ms, 64 × 64 matrix, 192 × 192 mm FOV, 30 × 3 mm slices, no gap, i.e. 3 mm isovoxel resolution).

Data analysis was conducted using BrainVoyager (Brain Innovation, Maastricht, The Netherlands). All functional data were slice-time corrected, motion corrected, and spatially/temporally bandpass filtered at 1–16 Hz/3–32 Hz, respectively (where spatial Hz refers to cycles/image matrix and temporal Hz refers to cycles/run length). Retinotopic maps were produced by correlating each stimulus location in the visual field with the change in intensity over time for

each voxel in the functional data [16]. Specifically, for each stimulus location: (1) the hemodynamic response function (HRF) was modeled using a gamma function [17] (with $\delta = 2.5$ and $\tau = 1.25$), (2) this model was cross-correlated with every voxel in the functional data, and (3) voxels with a correlation coefficient above a threshold value were painted a color associated with that stimulus position (see color wheel in Fig. 3). For all retinotopic maps shown, a correlation threshold of 0.20 was used.

Segmentation and surface reconstruction of the anatomic volume was conducted using methods similar to those described elsewhere [7,9,18–22] with subsequent cortical surface inflation to assist in viewing activation patterns (for specific details see [23]). Retinotopic maps were projected onto the cortical surfaces and borders between visual areas identified, when possible, by assuming field sign inversion (i.e. color reversals) in adjacent visual areas [7,9,24].

For reference purposes, the retinotopic map of a normal control subject is shown in Fig. 3. Human retinotopic maps are consistently organized regarding their location relative to anatomic landmarks and topographic organization. In particular, a representation of the right horizontal meridian (HM, i.e. the line dividing the upper and lower visual field) is mapped onto left hemisphere V1 near the base of the calcarine sulcus and additional HM representations are mapped roughly parallel to the V1 HM representation but offset in both the dorsal and ventral directions. Field sign

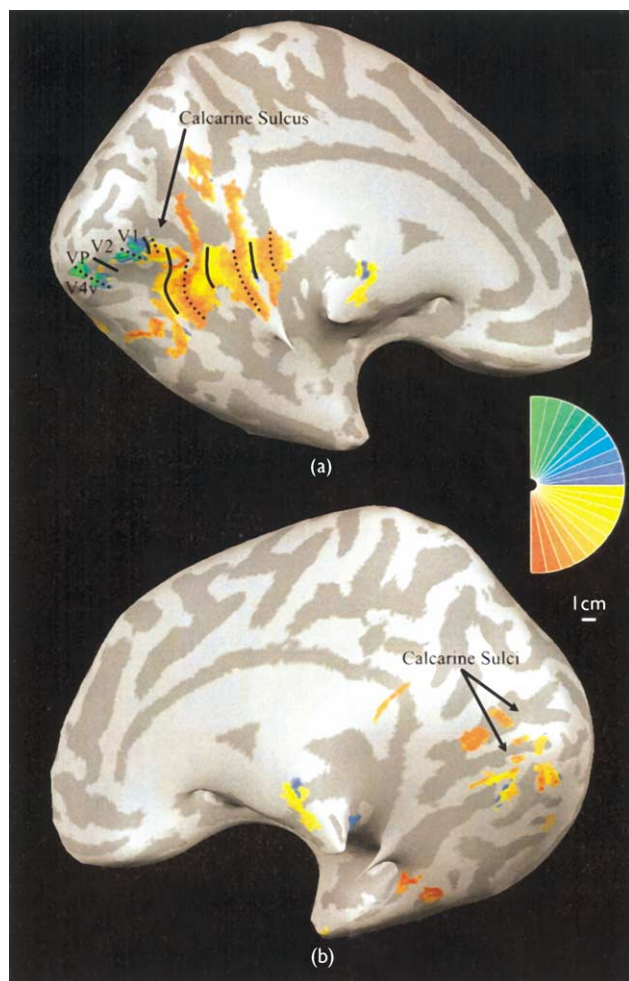


Fig. 4. (a) Retinotopic map of right visual field projected onto inflated left hemisphere of the patient. Ventral visual areas, representing the upper right quadrant of the visual field, and displaced dorsal visual areas/borders, representing the lower right quadrant of visual field, were labeled using field sign inversion. (b) Retinotopic map of right visual field projected onto inflated right hemisphere of the patient.

inversion in adjacent visual areas can readily be observed by the smooth yellow-to-red color transition extending from the V1 HM to the lower vertical meridian (LVM) at the dorsal V1-V2 border, the red-to-yellow color transition from the dorsal V1-V2 border to the dorsal V2-V3 border, etc. It is also important to note that stimulation of the right visual field normally elicits activity in the left hemisphere only. Stimulation of the left visual field results in the mirror reversal of the retinotopic map described above.

RESULTS

Although somewhat disjointed, the organization of the patient's left hemisphere ventral visual areas, corresponding to stimulation in the upper right quadrant of the visual field, was largely normal (Fig. 4a). In particular, the V1 HM was mapped near the base of the calcarine sulcus and the upper vertical meridian representations separating ventral V1/V2

and VP/V4v could be identified and were offset in the ventral direction.

In contrast, the patient's left hemisphere dorsal visual areas, corresponding to stimulation in the lower right quadrant of the visual field, were atypically organized. Fig. 4a shows that visual borders/areas corresponding to stimulation of the lower right quadrant of the visual field were located on the medial surface of the left hemisphere rather than their typical location dorsal and parallel to the V1 HM (compare Fig. 4a and Fig. 3b). In addition, there were at least 4 unique representations of both horizontal and vertical meridians which, if field sign inversion is assumed to separate unique visual areas, define at least 8 early visual areas (compared to four normally observable visual areas). Figure 4b illustrates additional right hemisphere visual area activation corresponding to lower right visual field stimulation, which normally shows no activation by stimuli presented in this hemifield. Although there was significant displacement and expansion of visual areas, both within and across hemispheres, contralateral visual field inversion in adjacent visual areas appeared to be largely conserved. In other words, the smooth transitions from yellow-to-red, red-to-yellow, and so on, are consistent with the functional architecture of normal visual field representation.

As can be observed in Fig. 5, the map corresponding to left visual field stimulation had no apparent retinotopic organization. In fact the left visual field was mapped onto numerous small islands on both left and right hemispheres.

DISCUSSION

Although the retinotopic map of the upper right visual field on the ventral left hemisphere was largely normal in both location and organization, the retinotopic map of lower right visual field was shifted in location relative to normal. In a normal retinotopic map field sign reversals are assumed to define the borders between visual areas. If this assumption is correct, this patient had twice as many retinotopically organized early visual areas allocated to lower right visual field when compared to normal (compare Fig. 3b and Fig. 4a). Still, the overall organization, i.e. visual field sign reversals, was normal and as such illustrates a large-scale shift in location only.

The most focal aspect of the patient's dysgenesis was restricted to the right hemisphere (Fig. 1b,c). This right hemisphere dysgenesis included an area of abnormal cortical migration that disrupted white matter tracts normally carrying retinotopic input from the left visual field. Such atypical neural organization may have caused the retinotopic map to fragment and remap onto multiple islands of spared cortex in both hemispheres (i.e. a shift in both location and topography, Fig. 5). The remapping of the left visual field onto left hemisphere dorsal extrastriate cortex (Fig. 5a) may have contributed to the large-scale shift of the left hemisphere dorsal retinotopic map of the right visual field as discussed above. We cannot rule out the possibility that this shift was due in full or part to the global dysgenesis of the left hemisphere. However, both the relatively normal organization of left hemisphere ventral retinotopic map and the fact that the dorsal cortical dysgenesis is similar to the ventral cortical dysgenesis

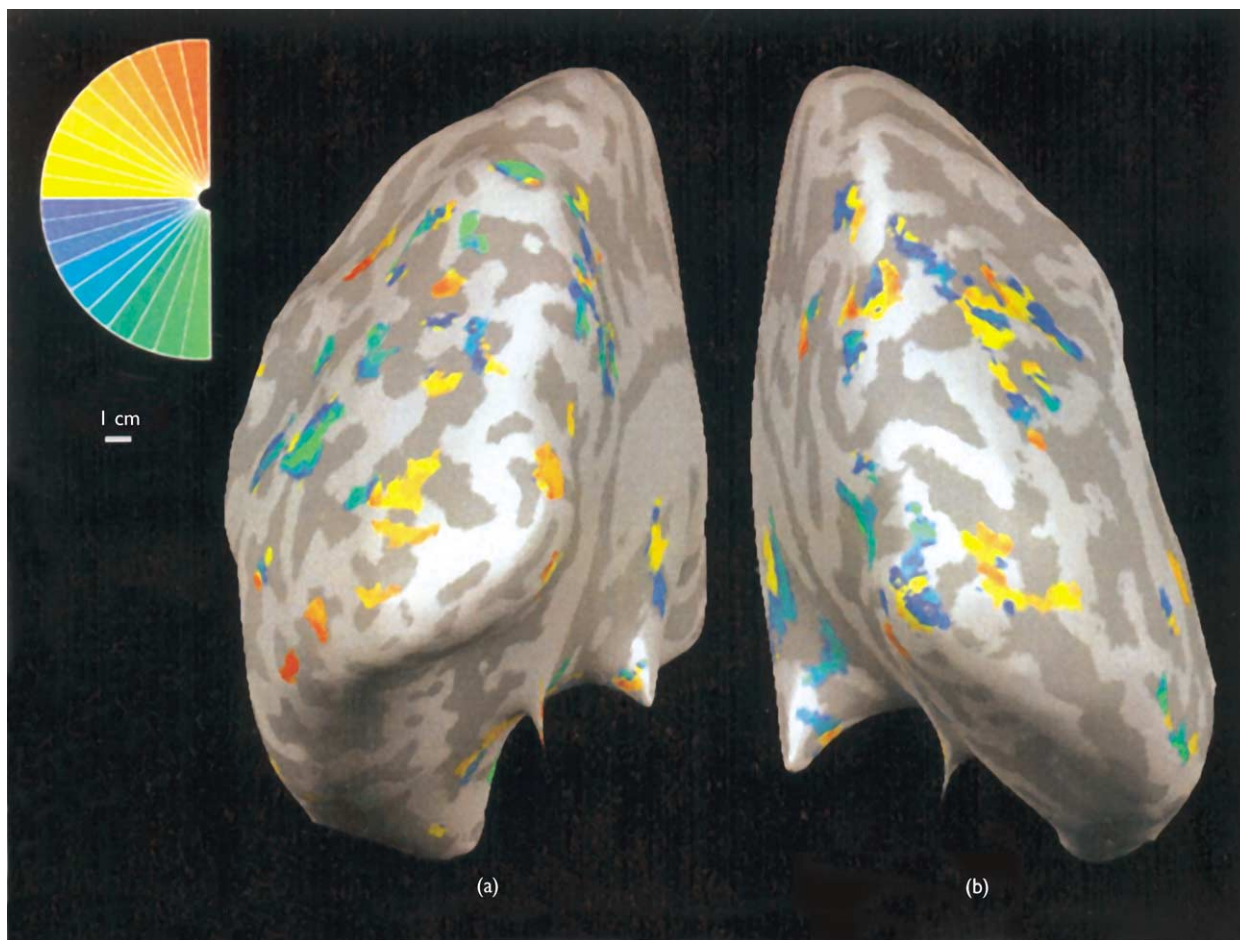


Fig. 5. Retinotopic map of left visual field projected onto inflated hemispheres. Hemispheres were rotated to maximize the observable cortical activation, resulting in a nearly direct posterior viewing angle (as if looking at the back of the patient's brain). (a) Left hemisphere. (b) Right hemisphere.

(compare Fig. 1b and Fig. 1d), would argue against this possibility and in favor of functional displacement of the left hemisphere dorsal retinotopic map by the remapped left visual field representation.

This case study is illustrative of two of the hypotheses put forth in the introduction. Specifically, the retinotopic map corresponding to one quadrant showed a shift in location with spared topography and the retinotopic map corresponding to an entire visual hemifield was shifted in both location and topography. Detailed perimetry mapping did not reveal any visual field deficits; therefore, our results are inconsistent with the hypothesis that retinotopic maps are fixed in their cortical location.

CONCLUSION

Although retinotopic maps are highly stable across normal individuals regarding their location relative to anatomic landmarks and topographic organization, this case illustrates that large-scale reorganization is possible. Moreover, this reorganization has been shown to take two forms, one involving a shift in location with spared topography and the other involving a shift in both location and topography.

This case study illustrates the diverse capacity of cortical reorganization with the presumed aim of functional preservation.

REFERENCES

- Seitz RJ, Huang Y, Knorr U *et al.* *Neuroreport* **6**, 742–744 (1995).
- Wunderlich G, Knorr U, Herzog H *et al.* *Neurosurgery* **42**, 18–26 (1998).
- Alkadhi H, Kollias SS, Crelier GR *et al.* *Am J Neuroradiol* **21**, 1423–1433 (2000).
- Lazar RM, Marshall RS, Pile-Spellman J *et al.* *Neuropsychologia* **38**, 1325–1332 (2000).
- Vikingstad EM, Cao Y, Thomas AJ *et al.* *Neurosurgery* **47**, 562–570 (2000).
- Sadato N, Pascual-Leone A, Grafman J *et al.* *Nature* **380**, 526–528 (1996).
- Sereno MI, Dale AM, Reppas JB *et al.* *Science* **268**, 889–893 (1995).
- DeYoe EA, Carman GJ, Bandettini P *et al.* *Proc Natl Acad Sci USA* **93**, 2382–2386 (1996).
- Tootell RBH, Mendola JD, Hadjikhani NK *et al.* *J Neurosci* **17**, 7060–7078 (1997).
- Engel SA, Glover GH and Wandell BA. *Cerebr Cortex* **7**, 181–192 (1997).
- Morland AB, Baseler HA, Hoffman MB *et al.* *Acta Psychol* **107**, 229–247 (2001).
- Logothetis NK, Pauls J, Augath M *et al.* *Nature* **412**, 150–157 (2001).
- Rees G, Friston K and Koch C. *Nature Neurosci* **3**, 716–723 (2000).

14. Heeger DJ, Huk AC, Geisler WS and Albrecht DG. *Nature Neurosci* **3**, 631–633 (2000).
15. Slotnick SD, Klein SA, Carney T *et al.* *Clin Neurophysiol* **112**, 1349–1356 (2001).
16. Goebel R, Muckli L, Zanella FE *et al.* *Vision Res* **41**, 1459–1474 (2001).
17. Boynton GM, Engel SA, Glover GH *et al.* *J Neurosci* **16**, 4207–4221 (1996).
18. Dale AM and Sereno MI. *J Cogn Neurosci* **5**, 162–176 (1993).
19. Drury HA, Van Essen DC, Anderson CH *et al.* *J Cogn Neurosci* **8**, 1–28 (1996).
20. Van Essen DC and Drury HA. *J Neurosci* **17**, 7079–7102 (1997).
21. Dale AM, Fischl B and Sereno MI. *Neuroimage* **9**, 179–194 (1999).
22. Fischl B, Sereno MI and Dale AM. *Neuroimage* **9**, 195–207 (1999).
23. Linden DEJ, Kallenbach U, Heinecke A *et al.* *Perception* **28**, 469–481 (1999).
24. Sereno MI, McDonald CT and Allman JM. *Cerebr Cortex* **4**, 601–620 (1994).

Acknowledgements: S.D.S. is supported by post-doctoral training grant MHI9971 in perceptual and cognitive neuroscience from the NIMH. This work was supported in part by NIH/NCRR grant P41 I5241 to J.H.